A solution of Maxwell's equations for the proton mass

R. H. Dishington

P. O. Box 333
Pacific Palisades, CA
90272

October 2003

Abstract

It is generally agreed that the principal factor missing from the Standard Model is the ability to calculate the particle masses. The available method for handling the "point" leptons also can lead to difficulties. The following presents an approach to these two problems by finding a simple, finite solution of Maxwell's equations that applies to all leptons except photons and neutrinos.

The "point" quarks in the Standard Model are replaced by these finite components, and the structure and rest energy (mass) of the proton are calculated rigorously and exactly, from scratch; using only measured data from the leptons e, μ and τ.

I. INTRODUCTION

Around 1900, the search was on for a purely electromagnetic solution of Maxwell's equations to describe the electron and the few other known particles. This did not work out. Both then and now, the most popular solution has been the "point" charge, with its infinities and other complications. At present, with hindsight, it is possible to replace the "point" charge with a simple, finite solution of Maxwell's equations that appears to describe all leptons except photons and neutrinos. When the "point" quarks of the Standard Model are replaced by these finite components, the 1900 particle structure goal of Abraham, Lorentz, Einstein, Mie, etc. is attainable.

Using the finite lepton solution, an energy compaction relationship is derived, in the form $E_0 r_i = e^2/32\pi$ (Heaviside-Lorentz units throughout), for leptons with charge $\pm e$; where E_0 (ergs) and r_i (cm) are the rest energy and effective lepton radius respectively, and e is in hlcoulombs.

Next, the measured energies of the leptons with charge $\pm e$ are used with the energy compaction relationship to determine the leptons' effective radii. Being the simplest, whole charge particles, these are considered as *preferred states* of the vacuum, and these *preferred* radii are later shown to be preserved in the structures of mesons and baryons.

Finally, the finite Maxwell's equation solution is applied to multiple layer particles, and a generalized solution is provided. This formalism is used to calculate the three component self energies and three interaction energies of the proton, starting only with the charge/layer configuration. No proton measurements are used in the calculation, only the three "preferred" radii found from the e, μ and τ leptons. *The final calculated energy is the same as the measured rest energy of the proton.*

Conclusions are drawn about particle structure in general.

II. A FINITE PARTICLE SOLUTION OF MAXWELL'S EQUATIONS

A solution of the scalar equation (Heaviside-Lorentz units),

$$\nabla^2\phi = -\rho \quad , \tag{1}$$

must be found that eliminates the infinities of the "point" charge. A simple, spherical *trial* solution is,

$$\phi = \phi_0(1 - \psi^2) \quad ; \tag{2}$$

where ψ is the shape factor, $\psi = e^{-r_i/r}$. Figure 1 indicates that this potential has only two significant features, the center value ϕ_0 (positive or negative) and the radius r_i of the inflection point.

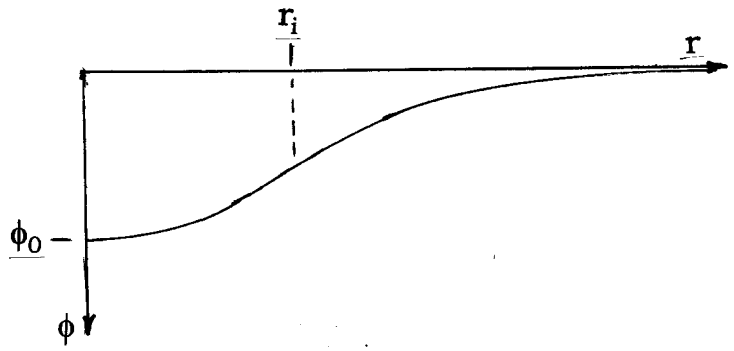

Figure 1

The corresponding charge density distribution required to complete the solution is found by substituting the *trial* solution Eq.(2) in Eq.(1) to yield,

$$\rho = 4\frac{\phi_0 r_i^2}{r^4}e^{-2r_i/r} \quad , \tag{3}$$

a smooth shell of charge distortion that peaks at *half* r_i. This distribution is a reasonable one. Integrated over all space, the total charge is $q = 8\pi\phi_0 r_i$.

Similarly, the electric energy density distribution is found from,

$$\varepsilon_e = \tfrac{1}{2}(\nabla\phi)^2 = 2\frac{\phi_0^2 r_i^2}{r^4}e^{-4r_i/r} \quad , \tag{4}$$

a smooth shell of energy distortion *that peaks at the inflection radius* r_i. If ε_e is integrated over all space, the resulting finite energy is $E_0 = 2\pi\phi_0^2 r_i$.

Just to get some idea of the magnitudes involved, if the potential in Eq.(2) is assumed to represent an electron, then using $E_0 = 8.18711\times10^{-7}$ergs (0.511 MeV) and $q = -e = -1.7027\times10^{-9}$hlcoul ($-1.6022\times10^{-19}$C), the center potential and inflection point radius are $\phi_0 = -1.9233\times10^{3}$hlvolts (approx. -2×10^{6}V) and $r_i = 3.522\times10^{-14}$cm.

It is important to notice that the expansion of the *gradient* of Eq.(2),

$$\frac{d\phi}{dr} = -2\frac{\phi_0 r_i}{r^2}\left(1 - 2\frac{r_i}{r} + 2\frac{r_i^2}{r^2} - \ldots\right) \qquad r > r_i$$

reduces, for the electron, to $d\phi/dr \cong e/4\pi r^2$ (for $r > 200r_i$), the Coulomb field of the "point" charge. This explains why the well known collision experiments[1] that appear to support the "point" charge electron model are also in complete agreement with the present, finite solution. At low collision energies, the principal interaction is out in the Coulomb region. As the collision energy is increased, the Lorentz contraction of the gradient causes the inner, non-Coulomb volume to shrink, and *the interaction never catches up with that inner region.*

III. THE ENERGY COMPACTION RELATIONSHIP

Combining the rest energy E_0 and charge q found from Eqs.(4) and (3), for whole charge leptons,

$$E_0 r_i = \frac{e^2}{32\pi} = 2.8838\times10^{-20}\,\text{erg}-\text{cm} \quad , \qquad (5)$$

a relationship called the energy compaction equation. It indicates that

---

1. D.P. Barker, et. al., Phys. Rev. Lett., **43**, 1915 (1979); Phys. Rev. Lett., **45**, 1904 (1980).

the more energetic leptons are smaller. The true importance of Eq.(5) appears when analyzing composite particles such as the proton.

Larger particles (mesons and baryons) are formed by combining components of the type shown in Figure 1, which can have individual radii that differ from one another. *The analysis depends upon identifying an effective radius* r_e*, of the combined components.* It appears that the energy compaction relationship of Eq.(5) is more general than might be thought, and *it applies to all whole charge particles, in the form,*

$$E_0 r_e = \frac{q^2}{32\pi} \quad , \tag{6}$$

where r_e is the whole composite particle's effective radius.

IV. LEPTONS

A. Lepton size and stability

Here, again, the leptons of interest will be limited to the series of whole charged particles, i.e. e, μ, τ, ..., that can exist alone and be observed for some finite time. Using the energy compaction relationship derived earlier, and the known values of E_0 for each of the leptons, the values for ϕ_0 and r_i are listed in TABLE I along with each particle's observed mean life.

TABLE I

LEPTONS, THE "PREFERRED" VACUUM STATES

	E_0 (ergs)	r_i (cm)	ϕ_0 (hlvolts)	mean life (s)
e	8.1871×10^{-7}	$r_1 = 3.5224\times10^{-14}$	1.9233×10^{3}	Stable
μ	1.6929×10^{-4}	$r_2 = 1.7035\times10^{-16}$	3.9768×10^{5}	2.1970×10^{-6}
τ	2.8472×10^{-3}	$r_3 = 1.0129\times10^{-17}$	6.6886×10^{6}	2.9100×10^{-13}

The interesting features of TABLE I are that, first, although each of these leptons has the same charge $\pm e$, the more energetic particles have higher potentials; and, their energy being packed into a smaller volume correlates with their being less stable. Second, it appears that the lepton sequence is a set of *preferred* states that can exist because of some fundamental property of the vacuum. Later on, in analyzing the more massive, composite particles, it is apparent that there are at least two more *preferred* states, 4 and 5; but their great compactness and instability may make their existence possible only inside the composite particles and not observable as leptons of higher order.

B. Quarks

From the 1960's on, it has been understood that the more elaborate particles are constructed of objects, now called quarks, that sometimes behave in a manner similar to leptons but have fractional charges $\pm e/3$ and $\pm 2e/3$. They are thought to be "point" charges like the conventional electron model. *Little is known about the spatial arrangement of these objects inside a composite particle*.

In interactions between quarks and external projectile particles*, the quarks behave as if they were independent entities, but no individual quark has ever been observed outside its housing particle*. This suggests that the composite particles might be made up of very flexible constructs similar to the finite leptons described earlier, but having fractional charges, two components for the mesons and three for the baryons. In that case, although the components might freely move for short distances, if one of the components were forced out of a composite particle, because of its fractional charge it would not qualify as one of the preferred lepton solutions of Eq.(1) listed in TABLE I, and so would decay; as would the remaining debris from the original particle. If this is a correct description of composite particles, then all of the properties of

the Standard Model are preserved and yet a greater flexibility results.

V. PARTICLE CLASSIFICATION

The classification scheme described here includes all whole charge particles, but not photons and neutrinos. Using the Standard Model as a guide, the two "point" quarks that make up mesons and the three "point" quarks that make up baryons are replaced with the finite solutions of Figure 1. To avoid confusing the properties of the "point" quarks with these constructs, the term quark will not be used to describe the particle components.

Whereas the quarks have specific charges assigned, the present scheme first indicates only the number of components a particle has. For example, the leptons listed in TABLE I are single potential structures called *unons* and symbolized by U_i, where the subscript identifies the size and shape of the component (see TABLE I).

The mesons or *bions* have two components and are symbolized by B_{ij} $(i \le j)$; and the baryons or *trions* have three components symbolized by T_{ijk} $(i < j < k)$. In all these cases, *the Figure 1 constructs take on only the preferred radii listed in TABLE I*, so the subscripts indicate the size and shape of the components. For example, the proton will be shown to have the structure T_{123}; i.e. a component ϕ_1 with energy radius r_1, a larger component ϕ_2 with smaller energy radius r_2 and a very large component ϕ_3 with a still smaller energy radius r_3. On the other hand, there could be another trion T_{245} with components ϕ_2, ϕ_4 and ϕ_5 and energy radii r_2, r_4 and r_5. Only those "preferred" radii given in TABLE I and the possible r_4 and r_5, still to be determined accurately, ever appear in the components of multiple particles. For now, only educated guesses of the energies and radii of possible components 4 and 5 are available.

The increased flexibility of this system comes from the fact that the *fractional charges* of each component have yet to be specified. Now it appears that *all independent, observable particles have total charges that are integral multiples of e*. Because of this empirically determined fact, it is convenient to set up the next step in the classification system on the basis of the smoothed out charge shell of Eq.(3) rather than the potential of Eq.(2) or the energy shell of Eq.(4) , since the total integrated charge of any shell is constant, even when the particle is in motion. For example, the proton will be identified as the trion T^{-++}_{123}, where the superscripts indicate that the fractional charges of the components are $-e/3$, $+2e/3$, $+2e/3$. The neutron has been tentatively identified as T^{-+-}_{123}.

Bions are classified into three groups:

1. Concentric shell bions
2. Eccentric shell, inside orbiters

} B_{ij}

3. Outside orbiters B_{ii}

Group 1 bions have two shells, one inside the other, with a common center. Group 2 bions have two shells, one inside the other, with centers displaced and both orbiting a common center. Group 3 bions, like positronium, have two separate, equal, opposite charge shells, orbiting a common center. Observed concentric bions are tentatively identified as $\pi^{\pm}, D^{\pm}, D_s^{\pm}$ and $B^{\pm}$. Inside orbiter bions are probably K^0, D^0, B^0 and B_s^0, and outside orbiter bions are most likely $\pi^0, \eta, \eta', \eta_c$ and Υ. The latter decay like positronium and, similarly, produce two photons.

All bions are unstable. Thus, their correct analysis must address the transient case, which has many mathematical difficulties. Therefore, the measured bion energies are always slightly smaller than the values calculated from the "concentric, static" approximation.

The trions come in combinations of concentric shells, or eccentric inside orbiters. Although work is in progress, the only exactly calculable

concentric trion at this time is the stable proton. The great majority of trions appear to be inside orbiters, none of which has been finally identified yet due to mathematical intractability. The success of the proton analysis demands that the much more difficult problem of the orbiter trions be pursued, particularly that of the neutron.

VI. PARTICLE ANALYSIS

A. Multiple layer particles

The proton will be analyzed here, but it is straightforward to generalize the process for any concentric particle. The principal idea is that *the only physical presence is the sum of the potentials* ϕ_i *of its layers,*

$$\phi = \phi_1 + \phi_2 + \phi_3 + \ldots\ldots \quad , \tag{7}$$

where,

$$\phi_i = \phi_{0i} - \frac{q_i}{4\pi r_e} I_i(r) \quad , \tag{8}$$

and,

$$I_i(r) = r_e \int_0^r \frac{\psi_i^2}{r^2} dr \quad . \tag{9}$$

If the layer energies added in a similar fashion, the task would just involve the sum of those energies. However, when two or more layers are combined, there is "interaction" energy between each pair, and the energy density for the proton is,

$$\varepsilon_e = \tfrac{1}{2}(\nabla\phi)^2 = \tfrac{1}{2}(\nabla\phi_1)^2 + \tfrac{1}{2}(\nabla\phi_2)^2 + \tfrac{1}{2}(\nabla\phi_3)^2 + \nabla\phi_1 \bullet \nabla\phi_2 + \nabla\phi_1 \bullet \nabla\phi_3 + \nabla\phi_2 \bullet \nabla\phi_3 \tag{10}$$

Integrating Eq.(10) over all space gives the total particle energy as,

$$E_0 = E_1 + E_2 + E_3 + E_{12} + E_{13} + E_{23} \quad , \tag{11}$$

where the E_i are the layer self energies and the E_{ij} are the interaction energies. The next step is to determine how the interaction energies affect the particle's effective radius r_e. Clearly, the simple unon shape factors $\psi_i = e^{-r_i/r}$ cannot determine the radius of a *composite* particle. What is needed is a general solution of Eq.(1) that has the same form as Eq.(2) but more flexible shape factors.

It can be shown that the same trial potential of Eq.(2) with a modified shape factor,

$$\psi_i = e^{-\frac{r_e}{r}[1+K_i E_2(\frac{r}{r_e})]} \quad , \tag{12}$$

provides such a layer solution, with $E_2(r/r_e)$ representing the exponential integral of the second kind[2] and K_i an, as yet, undefined constant. For $K_i = 0$, the solution reduces to that of the unons. However, *in the multi-layer particles, each layer has a different value of* K_i that relates the *effective* radius r_e of the whole particle to the preferred energy radii of the layers, listed in TABLE I, through the expression,

$$K_i = \left(\frac{r_i}{r_e} - 1 \right) e^{r_i/r_e} \quad . \tag{13}$$

If a layer is very far out from the main energy of the particle, the K_i of that layer is a very large number. If a layer is close to r_e, K_i approaches zero. For a layer smaller than r_e, $-1 < K_i < 0$.

That Eq.(12) is a useful shape factor is supported by the fact that, when the layer charge densities,

$$\rho_i = \frac{q_i r_e}{2\pi} \left(1 + K_i e^{-r/r_e} \right) \frac{\psi_i^2}{r^4} \quad , \tag{14}$$

are integrated over all space, their charges are found to be independent

---

2. *Handbook of Mathematical Functions*, (National Bureau of Standards, AMS 55, p228).

of K_i. This is what makes the choice of layer charge for the classification scheme the most useful.

B. Energy calculations

From Eqs.(8) and (10), the various energies can be written,

$$E_i = \frac{q_i^2}{8\pi r_e} J_i(\infty) \quad , \quad J_i(r) = r_e \int_0^r \frac{\psi_i^4}{r^2}\, dr \quad , \tag{15}$$

and,

$$E_{ij} = \frac{q_i q_j}{4\pi r_e} J_{ij}(\infty) \quad , \quad J_{ij}(r) = r_e \int_0^r \frac{\psi_i^2 \psi_j^2}{r^2}\, dr \quad . \tag{16}$$

The integrals $I_i(\infty)$, in Eq.(9), and $J_i(\infty)$ have been evaluated numerically and tabulated, as functions of r_e, for rough calculations and also computerized, for more accurate calculations. For very large K_i, Eq.(13) goes out of range, so the integrals are found from,

$$I_i(\infty) \cong J_i(\infty) \to \frac{r_e}{r_i} \quad . \qquad \frac{r_i}{r_e} > 100$$

The interaction energies can be found by defining $K_{ij} = \frac{1}{2}(K_i + K_j)$. Then, from Eq.(13), an effective K is,

$$K_{ij} = \left(\frac{r_{ij}}{r_e} - 1 \right) \varepsilon^{r_{ij}/r_e} \quad ,$$

which can be used with the $J_i(r)$ integral table or computer calculation values to find $J_{ij}(\infty)$.

It should be noted that *Eqs.(6) and (11) are two independent equations in the two unknowns* E_0 *and* r_e, and both equations must be satisfied. Thus, once the charge/layer structure is specified, say T^{-++}_{123} in the case of the proton, by choosing a succession of values for r_e, and comparing the results from Eqs.(6) and (11), *the values of* E_0 *and* r_e *can be found without knowing them in advance.* However some care must be used in

these calculations. For example, in comparing the theory with the experimental data, it is *assumed* that the measured data give the true E_0 of the proton, i.e. $E_0 = 1.5033 \times 10^{-3}$ (938.27 MeV). Now, since Eq.(6) involves no approximations in calculating r_e, it is *assumed* that $r_e = 1.9183 \times 10^{-17}$ is the true effective proton radius. On the other hand, the calculations of the layer and interacting energies using Eq.(11) involves certain approximations in evaluating the energy integrals. Also, the simple quiescent model may be influenced by other conditions, such as the zero point fluctuations, and this should be kept in mind.

In the case of T^{-++}_{123}, the calculations using Eqs.(15) and (16) indicate that, for $r_e = 1.9183 \times 10^{-17}$ cm,

$$E_1 = 3.6387 \times 10^{-7} \quad , \quad E_2 = 2.5390 \times 10^{-4} \quad , \quad E_3 = 7.0631 \times 10^{-4}$$

$$E_{12} = -1.4555 \times 10^{-6} \quad , \quad E_{13} = -1.4555 \times 10^{-6} \quad , \quad E_{23} = 5.3612 \times 10^{-4}$$

When these energies are added together as in Eq.(11), $E_0 = 1.4938 \times 10^{-3}$ ergs (932.36 MeV), *which is just 0.63% lower than the measured rest energy of the proton.* No measurements of the proton were injected into the calculations.

If the E_0 vs. r_e curve, in the region where $r_e \geq 1..9183 \times 10^{-17}$, is computed using Eq.(11), the results are those listed in TABLE II. It crosses the E_0 curve found from Eq.(6) at $r_e = 1.9450 \times 10^{-17}$ cm, $E_0 = 1.4785 \times 10^{-3}$ ergs (922.81 MeV); but, by raising this curve at every point by 0.63%, the crossover point moves to the *measured* values. The

TABLE II

r_e	E_1	E_2	E_3	E_{12} & E_{13}	E_{23}	E_0
1.9183×10^{-17}	3.6387×10^{-7}	2.5390×10^{-4}	7.0631×10^{-4}	-1.4555×10^{-6}	5.3612×10^{-4}	1.4938×10^{-3}
1.9300×10^{-17}	3.6387×10^{-7}	2.5342×10^{-4}	7.0235×10^{-4}	-1.4555×10^{-6}	5.3553×10^{-4}	1.4888×10^{-3}
1.9400×10^{-17}	3.6387×10^{-7}	2.5317×10^{-4}	6.9873×10^{-4}	-1.4555×10^{-6}	5.3488×10^{-4}	1.4842×10^{-3}
1.9500×10^{-17}	3.6234×10^{-7}	2.5240×10^{-4}	6.9541×10^{-4}	-1.4578×10^{-6}	5.3319×10^{-4}	1.4785×10^{-3}

source of the 0.63% error is not yet known, but it is under investigation.

VIII. CONCLUSIONS

The theory has been extended far beyond this presentation, but it is too elaborate to easily organize for presentation. For example, the magnetic moments of the proton layers have been calculated and added in the proper orientation. They give an overall moment 5.6% lower than the observed value. However, a slight tilt of one of the layers raises the value to the one observed. With greater elaboration, many of the quantum mechanical properties of particles are understandable, but these must wait until the available material can be condensed.

The success of the stable proton analysis and the static approximation results for the concentric mesons lends credence to the system presented here. The inherent difficulty of the transient, inside orbiter analysis of the unstable baryons indicates that much remains to be done. Nevertheless, the results presented here point the way ahead.

ACKNOWLEDGMENT

The author wishes to acknowledge the considerable help on this problem rendered by R. L. Kirkwood, L. O. Heflinger, B. H. Mueller, D. J. Margaziotis, T. Hudspeth, R. S. Margulies and G. Ialongo.

UNITS

To obtain the quantity in HLU, multiply the MKS quantity by the factor given. To go from HLU to MKS, divide.

	HLU	MKS
Electric Potential	$\bar{\phi}$	9.40967×10^{-4} Volts
Magnetic Vector Potential	$\mathbf{A}$	2.82095×10^{5}
Energy	$\mathcal{E}$	10^{7} Joules
Energy Density	ε	10 Joules
Charge	q	1.06274×10^{10} Coulombs
Charge Density	ρ	1.06274×10^{4} Coulombs / m^3
Current	i	1.06274×10^{10} Amperes
Resistance	$\mathbb{R}$	8.85419×10^{-14} Ohms
Capacitance		1.12941×10^{13} Farads
Inductance	$\mathbb{L}$	8.85419×10^{-14} Henrys
Electric Intensity	$\mathbf{E}$	9.40967×10^{-6} Volts/m
Magnetic Induction	$\mathbf{B}$	2.82095×10^{3} Teslas
Electric Displacement	$\mathbf{D}$	1.06274×10^{6}
Magnetic intensity	$\mathbf{H}$	$3.54491 \times 10^{-3} \frac{\text{Amp Turns}}{\text{m}}$

UNITS

Starred quantities are Gaussian. Listed quantities are substituted directly. Quantities along rows are equal.

	HLU	MKS	EMU	ESU
Electric Potential	$\bar{\bar{\phi}}$	$\frac{10^8}{c_0\sqrt{4\pi}}\phi_{mks}$	$\frac{1}{c_0\sqrt{4\pi}}\phi_m$	$\frac{1}{\sqrt{4\pi}}\phi_s$ *
Magnetic Vector Potential	$\mathbf{A}$	$\frac{10^6}{\sqrt{4\pi}}\mathbf{A}_{mks}$		$\frac{1}{\sqrt{4\pi}}\mathbf{A}_s$ *
Charge	q	$\frac{c_0\sqrt{4\pi}}{10}q_{mks}$	$c_0\sqrt{4\pi}\ q_m$	$\sqrt{4\pi}\ q_s$ *
Current	i	$\frac{c_0\sqrt{4\pi}}{10}i_{mks}$	$c_0\sqrt{4\pi}\ i_m$	$\sqrt{4\pi}\ i_s$ *
Electric Intensity	$\mathbf{E}$	$\frac{10^6}{c_0\sqrt{4\pi}}\mathbf{E}_{mks}$	$\frac{1}{c_0\sqrt{4\pi}}\mathbf{E}_m$	$\frac{1}{\sqrt{4\pi}}\mathbf{E}_s$ *
Magnetic Intensity	$\mathbf{H}$	$\sqrt{4\pi}10^{-3}\mathbf{H}_{mks}$ (A.T./m)	$\frac{1}{\sqrt{4\pi}}\mathbf{H}_m$ *	$\frac{1}{c_0\sqrt{4\pi}}\mathbf{H}_s$
Electric Displacement	$\mathbf{D}$	$\sqrt{4\pi}10^{-5}c_0\mathbf{D}_{mks}$	$\frac{c_0}{\sqrt{4\pi}}\mathbf{D}_m$	$\frac{1}{\sqrt{4\pi}}\mathbf{D}_s$ *
Magnetic Induction	$\mathbf{B}$	$\frac{10^4}{\sqrt{4\pi}}\mathbf{B}_{mks}$ (Teslas)	$\frac{1}{\sqrt{4\pi}}\mathbf{B}_m$ *	$\frac{c_0}{\sqrt{4\pi}}\mathbf{B}_s$
Magnetic Moment	μ	$10^3\sqrt{4\pi}\ \mu_{mks}$	$\sqrt{4\pi}\ \mu_m$	$\frac{\sqrt{4\pi}}{c_0}\ \mu_s$ *
Conductivity	σ	$\frac{4\pi c_0^2}{10^9}\sigma_{mks}$	$4\pi c_0^2\ \sigma_m$	$4\pi\sigma_s$ *
Resistance	$\mathbb{R}$	$\frac{10^9}{4\pi c_0^2}\mathbb{R}_{mks}$	$\frac{1}{4\pi c_0^2}\mathbb{R}_m$	$\frac{1}{4\pi}\mathbb{R}_s$ *
Capacitance	$\mathbb{C}$	$\frac{4\pi c_0^2}{10^9}\mathbb{C}_{mks}$	$4\pi c_0^2\ \mathbb{C}_m$	$4\pi\mathbb{C}_s$ *
Inductance	$\mathbb{L}$	$\frac{10^9}{4\pi c_0^2}\mathbb{L}_{mks}$	$\frac{1}{4\pi c_0^2}\mathbb{L}_m$	$\frac{1}{4\pi}\mathbb{L}_s$ *

TRUNCATIION INTEGRALS

1. $\int_0^x \varepsilon^{-1/y} dy = T(x)$ The truncation integral.

2. $\int_0^x \varepsilon^{-a/y} dy = a\, T\left(\frac{x}{a}\right)$

3. $\int_0^x y\, \varepsilon^{-a/y} dy = \frac{x^2}{2}\varepsilon^{-a/x} - \frac{a^2}{2} T\left(\frac{x}{a}\right)$

4. $\int_0^x y^2 \varepsilon^{-a/y} dy = \left(\frac{x^3}{3} - \frac{ax^2}{2\cdot 3}\right)\varepsilon^{-a/x} + \frac{a^3}{2\cdot 3} T\left(\frac{x}{a}\right)$

5. $\int_0^x y^3 \varepsilon^{-a/y} dy = \left(\frac{x^4}{4} - \frac{ax^3}{3\cdot 4} + \frac{a^2x^2}{2\cdot 3\cdot 4}\right)\varepsilon^{-a/x} - \frac{a^4}{2\cdot 3\cdot 4} T\left(\frac{x}{a}\right)$

6. $\int_0^x y^n \varepsilon^{-a/y} dy = \left(\frac{x^{n+1}}{n+1} - \frac{ax^n}{n(n+1)} + \frac{a^2x^{n-1}}{(n-1)n(n+1)} - \cdots\right.$

$$\left. \cdots\cdots\cdots \pm \frac{a^{n-1}x^2}{(n+1)!}\right)\varepsilon^{-a/x} \mp \frac{a^{n+1}}{(n+1)!} T\left(\frac{x}{a}\right)$$

7. $\int_0^x \frac{\varepsilon^{-a/y}}{y^2} dy = \frac{\varepsilon^{-a/x}}{a}$

8. $\int_0^x \frac{\varepsilon^{-a/y}}{y^3} dy = \frac{\varepsilon^{-a/x}}{a^2}\left(1 + \frac{a}{x}\right)$

9. $\int_0^x \frac{\varepsilon^{-a/y}}{y^4} dy = \frac{2\varepsilon^{-a/x}}{a^3}\left(1 + \frac{a}{x} + \frac{a^2}{2x^2}\right)$

10. $\int_0^x \frac{\varepsilon^{-a/y}}{y^n} dy = \frac{(n\text{-}2)!\varepsilon^{-a/x}}{a^{n-1}}\left(1 + \frac{a}{x} + \frac{a^2}{2!x^2} + \frac{a^3}{3!x^3} + \cdots\cdots + \frac{a^{n-2}}{(n-2)!x^{n-2}}\right)$

11. $Q(x) = \varepsilon^{1/x} T(x)$, $T(x) = \varepsilon^{-1/x} Q(x)$

12. $\frac{dQ(x)}{dx} = 1 - \frac{1}{x^2} Q(x)$

x	T(x)	x	T(x)
0.05	4.7024×10^{-12}	7.00	4.5615
0.10	3.8302×10^{-7}	7.50	4.9971
0.15	2.2539×10^{-5}	8.00	5.4365
0.20	1.9929×10^{-4}	8.50	5.8794
0.25	7.9955×10^{-4}	9.00	6.3254
0.30	2.1277×10^{-3}	9.50	6.7742
0.35	4.4403×10^{-3}	10.0	7.2254
0.40	7.9190×10^{-3}	11.0	8.1345
0.45	1.2674×10^{-2}	12.0	9.0512
0.50	$1..8767 \times 10^{-2}$	13.0	9.9743
0.55	2.6207×10^{-2}	14.0	10.9029
0.60	3.4990×10^{-2}	15.0	11.8362
0.65	0.04508	16.0	12.7737
0.70	0.05645	17.0	13.7149
0.75	0.06903	18.0	14.6593
0.80	0.08279	19.0	15.6067
0.85	0.09766	20.0	16.5567
0.90	0.11361	25.0	21.3385
0.95	0.13057	30.0	26.1594
1.00	0.14850	35.0	31.0076
1.20	0.2288	40.0	35.8759
1.40	0.3214	45.0	40.7595
1.60	0.4241	50.0	45.6552
1.80	0.5351	55.0	50.5608
2.00	0.6532	60.0	55.4746
2.50	0.9734	65.0	60.3952
3.00	1.3207	70.0	65.3216
3.50	1.6881	75.0	70.2531
4.00	2.0709	80.0	75.1890
4.50	2.4660	85.0	80.1287
5.00	2.8710	90.0	85.0719
5.50	3.2842	95.0	90.0181
6.00	3.7044	100.0	94.9671
6.50	4.1304	$x \to \infty$, $T(x) \to x - \log_e x$	